The Polyelectrolyte Brush: Poor Solvent

R. S. Ross*

Department of Physics, University of California, Santa Barbara, California 93106

P. Pincus

Materials and Physics Departments, University of California,
Santa Barbara, California 93106

Received September 30, 1991; Revised Manuscript Received December 20, 1991

ABSTRACT: We investigate the end-grafted polyelectrolyte brush in the poor solvent regime of the corresponding neutral polymer system. Using Poisson–Boltzmann theory for the electrostatics and Flory–Huggins mean-field theory for the excluded-volume and van der Waals like monomer interactions, we find the existence of a first-order phase transition to a collapsed state for moderate to highly charged polyelectrolytes in the poor solvent regime. Irreversibilities in the disjoining pressure between planar-grafted surfaces are predicted. For polyelectrolytes grafted to spherical and cylindrical surfaces with small radii of curvature, the phase transition is predicted to become second-order in the infinite molecular weight limit. A phase diagram for the entire poor solvent regime is given.

I. Introduction

The structure and properties of uncharged polymers which are end-grafted to a solid surface in the presence of a good solvent have received a great deal of attention in recent years.[1-10] The chains are found to be extended with a brush height that is linearly proportional to the molecular weight of the polymers. More recently Halperin[11] and Zhulina et al.[12] have extended these studies to include the effects of solvent quality on the brush structure. These authors have shown that with decreasing solvent quality there is a *continuous* shrinking of the corona thickness, but with the height continuing to scale linearly with the molecular weight. The case of electrically charged polymers, polyelectrolytes, which are grafted to surfaces in the presence of polar solvents has also begun to receive some theoretical attention.[13-15] This situation has important applications to colloid control in aqueous environments such as occur in waste water treatment, enhanced oil recovery, etc. Until now, the investigations of polyelectrolyte brushes have emphasized the role of the electrostatic interactions in determining the structure and disjoining pressure between opposing brushes (as would obtain during a collision between two colloidal particles). However, polyelectrolytes generally have organic backbones which are insoluble in polar solvents;[16,17] the solubility is induced by the dissociation and hydration energies associated with the polar groups. The purpose of this paper is to consider the effects of solvent quality on the properties of polyelectrolyte brushes. In particular, we will show that a first-order brush-collapse phase transition may be induced by modification of the solvent quality (achieved by changing temperature or pH) and possibly as a function of ionic strength. (While this paper was under preparation we received a preprint[18] of a manuscript by the Leningrad group where the same first-order transition is also discussed in the context of polyamphylytes, i.e., polyelectrolytes containing both positive and negative charges.) Indeed this phase transition in the brush structure is quite analogous to the collapse transition observed by Tanaka and his co-workers[19,20] in polyelectrolyte gels.

The organization of this paper is as follows. In the remainder of this Introduction, we recall the principal results of Halperin[11] and Zhulina et al.[12] on the dependence of the brush height on solvent quality for uncharged polymers. In section II we discuss a mean-field analysis of the corresponding structure for planar polyelectrolyte brushes. We make contact with the recent work of Borisov et al.[18] and develop a phase diagram for the polyelectrolyte brush in terms of the degree of neutralization and temperature. The disjoining pressure between two identical polyelectrolyte brushes is considered in section III. We provide an extension of our theory in section IV to the case of polyelectrolytes grafted to spherical and cylindrical surfaces whose radii of curvature are much smaller than typical layer dimensions. Finally some concluding remarks are made in the final section with some emphasis on irreversible behavior that might be expected and the effects of added electrolyte.

In order to understand the role of elasticity for macromolecules grafted to interfaces, we shall briefly review the principal points for the situation of end-grafted neutral polymers in contact with solvents of varying quality. The planar geometry is sketched in Figure 1. We consider the simple case of monodisperse polymers of degree of polymerization N, with a fixed mean grafting density,[21] d^{-2}. The solvent quality is described in terms of the Flory–Huggins free energy per unit volume for a semidilute solution[21] of the polymers in the same solvent[22]

$$Fa^3/T = -\frac{1}{2}\tau\phi^2 + \frac{1}{6}w\phi^3 + ... \qquad (I.1)$$

where a is a monomer dimension; τ is the dimensionless excluded-volume parameter, which is negative for good solvents and positive for poor solvents; ϕ is the polymer volume fraction;[23] and w is the third virial coefficient which is typically positive and of order unity. The polymers are extended in the form of a brush of thickness L, which is determined by balancing the excluded-volume repulsion tending to swell the chains against the entropic polymer elasticity. In mean-field theory the osmotic pressure, P, corresponding to a local monomer volume fraction, ϕ, is

$$P = \phi\left(\frac{dF}{d\phi}\right) - F = \frac{T}{a^3}\left(-\frac{1}{2}\tau\phi^2 + \frac{1}{3}w\phi^3 + ...\right) \qquad (I.2)$$

If a Gaussian polymer has an end-to-end length L, it stores an elastic energy $^1/_2kL^2$, where the elastic constant, k, for a random walk chain is $k \simeq T/Na^2$. Then, assuming that all of the grafted chains are stretched by an identical length

0024-9297/92/2225-2177$03.00/0

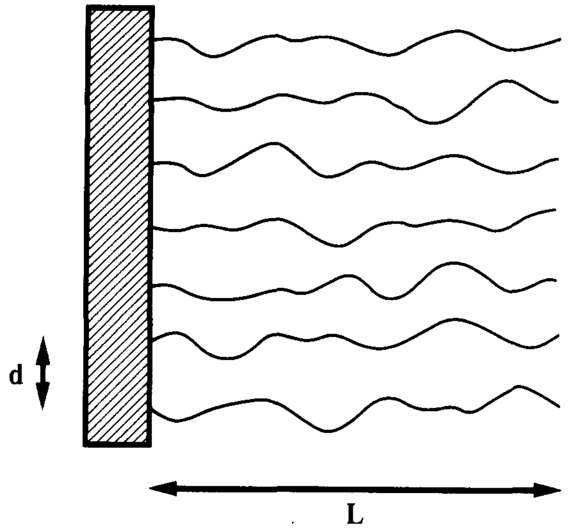

Figure 1. Schematic representation of the neutral polymer brush. The brush height is L; the mean grafting spacing is d.

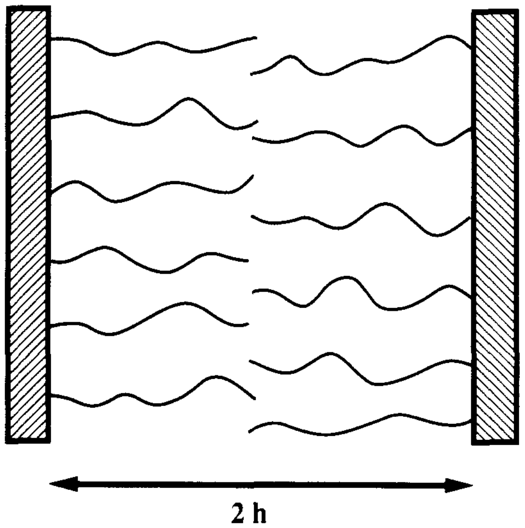

Figure 2. Schematic representation of two opposing neutral polymer brushes. The separation is $2h < 2L$.

L, static equilibrium is governed by

$$P = kL/d^2 \tag{I.3}$$

If the monomers are uniformly distributed[24] through the brush region, $\phi = Na^3/Ld^2$. There are several regimes depending on the magnitude of τ relative to w and the entropic elasticity. Assuming that w is of order unity, the three solvent quality regimes are as follows: good solvent, $\tau \le -(a/d)$; Θ solvent, $-(a/d) \le \tau \le (a/d)$; poor solvent, $\tau \ge (a/d)$. For good solvents, the third virial term is irrelevant and the brush height is given by the standard Alexander result, $L_g \simeq Na|\tau|^{1/3}(a/d)^{2/3}$. In the Θ regime, the balance is between the three-body interactions and polymer elasticity to yield $L_\Theta \simeq Na(a/d)$. For poor solvents, the elasticity is not relevant and the monomer concentration within the brush is determined by equilibration of the two- and three-body forces to give $L_\tau \simeq N a \tau^{-1}(a/d)^2$. It is important to note that the crossovers between these regimes are smooth and that there are no phase transitions in agreement with Zhulina et al.[12]

When two identical opposing brushes, Figure 2, approach one another with a separation $2h$, there is a contribution to the disjoining pressure that is associated with the polymer coronae when $h \le L$. This contribution, Π, is given by eq I.2 where the relevant volume fraction, ϕ, is given by $\phi = Na^3/d^2h$. For good solvents and weak compression, $h > Na^3/|\tau|d^2 = L_\tau$, the third virial term is negligible, and we find the standard Alexander scaling result[5]

$$\Pi_{\mathrm{g}} \simeq T\frac{N^2|\tau|a^3}{2d^4h^2} \tag{I.4}$$

In the Θ and poor solvent regimes, the disjoining pressure is

$$\Pi \simeq T\frac{N^3}{3d^4h^3}\left(1 - \frac{3}{2}\frac{\tau d^2}{N}h\right) \tag{I.5}$$

There is a continuous crossover from a h^{-2} dependence in good solvent to a h^{-3} dependence in poor solvent. Note, however, that at high compressions, $h < L_\tau$, the disjoining pressure is $\Pi \sim h^{-3}$, independent of solvent quality.

With this background, we are now in a position to consider the case of grafted polyelectrolytes where the solvent is of poor quality for the polymer backbone. The next section is devoted to a mean-field analysis of the brush structure.

II. Planar Brush Structure

We now extend the results of the last section for the solvent quality dependence of neutral brush structure to the case of grafted polyelectrolytes. The essential ingredient of this work is to explicitly include in the calculation of the equilibrium brush structure, effects arising from the insolubility of most hydrocarbon backbones in polar solvents.[16,17]

In the appendix we provide details of the calculation of the electrostatic free energy of an Alexander profile polyelectrolyte brush treated using Poisson–Boltzmann mean-field theory, as considered by Pincus.[15] We note that a similar model has also been recently considered by Borisov et al.[18] in which the electrostatics are treated in the Debye–Hückel approximation. Our appendix provides validation for this level of treatment. In the limits where our models coincide, i.e., no salt and only one sign of charge on the chains, we find equivalent results. In this work we restrict our attention to the following: (i) relatively high grafting densities where d is smaller than the free polymer radius of gyration (brush regime of the corresponding neutral system); (ii) the strong charging limit[15] in which the screening counterions are mainly confined to the polymer layer, $\kappa L \gg 1$, where κ is the self-consistent inverse Debye screening length in the brush volume, Figure 3. It is assumed that the solvent has been cleansed of free (ungrafted) polymer and is salt-free. We will comment on the addition of electrolyte in the Conclusion.

If f represents the fraction of monomeric units that are ionizable, we find (see the appendix) that in the strong charging regime, limited by $f > (d^2/N^2la)^{2/3}$ (satisfied for all but the smallest charge fractions), the Debye screening length is much smaller than the brush thickness L and the counterions are confined to the polymer layer. The dominant contribution to the electrostatic energy is the cost in entropy to localize the counterions $F_{\mathrm{es}}/T \simeq f\phi \ln(f\phi)$, where $f\phi = fNa^3/Ld^2$ is the mean counterion density fixed by local charge neutrality and mass conservation. We have taken the microscopic counterion volume as identical to the monomer dimension for simplicity. Solubility of the polymer backbones is taken account of in the mean-field approximation through Flory–Huggins terms as was done for the neutral brush in the Introduction, eq I.1. We include both the second and third virial terms since the primary interest is the poor solvent regime

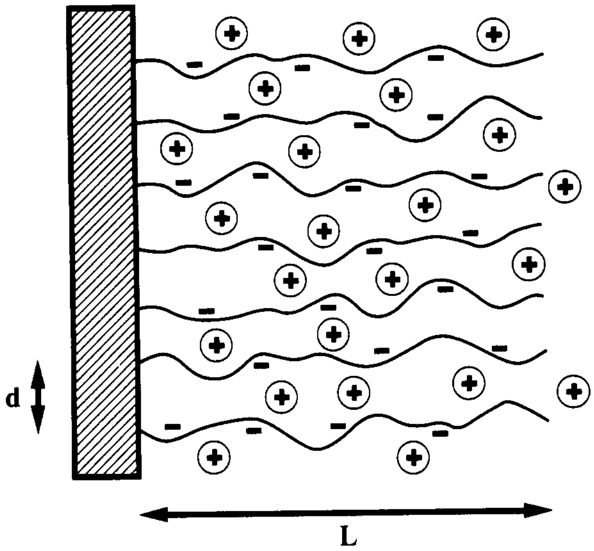

Figure 3. Schematic representation of a polyelectrolyte brush in the strong charging regime. The counterions (circled) are localized within the brush.

characterized by a negative excluded-volume parameter. The third virial term then is the lowest-order repulsive contribution to the swelling osmotic pressure. We finally assume as before that individual chains in the brush possess Gaussian elasticity.

In terms of the local monomer volume fraction ϕ, the free energy density of the polyelectrolyte brush then takes the form

$$\frac{Fa^3}{T} = f\phi \ln \phi - \frac{1}{2}\tau\phi^2 + \frac{1}{6}\phi^3 + \frac{L^2}{2Na^2}\frac{a^3}{Ld^2} \qquad \text{(II.1)}$$

where the first term is the entropy of mixing of the confined counterions, the middle two terms are the second and third virial terms, respectively, and the last term represents polymer Gaussian elasticity. We have assumed in writing the Flory–Huggins terms that the charge fraction is not so great so as to reduce significantly the number of bare monomer interactions. Indeed we will find that excluded-volume effects only play a significant role at very moderate values of the charge fraction, supporting the validity of this assumption.

Using the step-function profile $\phi = Na^3/Ld^2$, the free energy per unit area becomes

$$\frac{\gamma}{T} = \frac{F}{T}L = \frac{N}{d^2}\left(f \ln \phi - \frac{1}{2}\tau\phi + \frac{1}{6}\phi^2 + \frac{1}{2}\left(\frac{a}{d}\right)^4\phi^{-2}\right) \qquad \text{(II.2)}$$

Analysis of this effective scalar-field theory, in which the field ϕ is proportional to the inverse brush height L^{-1}, yields a very rich phase diagram. We present the phase diagram, Figure 4, for the polyelectrolyte brush in the τ–f plane for a fixed grafting density d^{-2}. Only the poor solvent regime is shown for which $0 < \tau < 1$. We find a line of first-order phase transitions roughly obeying $f^* \simeq (3/16)\tau^2$ terminating at a second-order critical point $f_c = 2(a/d)^2$, $\tau_c = (16/3\sqrt{3})(a/d)$. The critical volume fraction is found to be $\phi_c = \sqrt{3}(a/d)$.

At high charging $f > f_c$ and weak excluded-volume $\tau^2 < f^*$, the brush is in the typical polyelectrolyte regime.[15] The conformation is determined by the balance of electrostatic energy and polymer elasticity.

$$L_p = f^{1/2}Na \qquad \text{(II.3)}$$

Excluded-volume effects are too weak to play a significant role. This is the regime discussed originally by Pincus.[15]

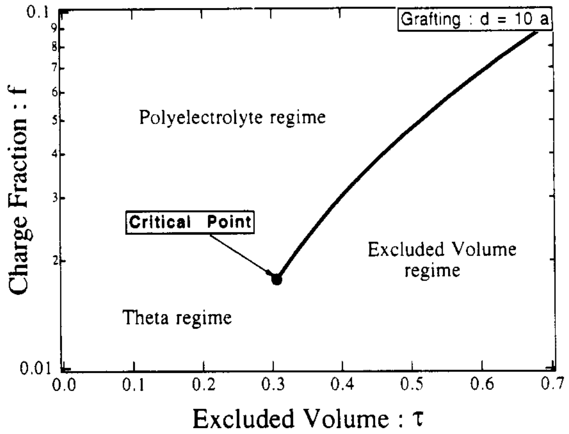

Figure 4. Phase diagram for the polyelectrolyte brush in the τ–f plane. The line of first-order transitions roughly obeys $f^* \simeq (3/16)\tau^2$. This phase diagram is fixed for a given grafting density d^{-2}, independent of N.

In the limit of very small charge fractions, $f < f_c$, and weak excluded-volume interactions, $\tau < \tau_c$, the brush is in the Θ regime, where three-body interactions dominate over electrostatics (counterion entropy) in balancing elasticity.

$$L_\Theta = Na(a/d) \qquad \text{(II.4)}$$

exactly as for the neutral brush. For higher excluded-volume energy, $\tau > \tau_c$, and relatively weak charging, $f^{1/2} < \tau^*$, the brush remains in the excluded-volume-dominated collapsed state.

$$L_\tau = Na(a/\tau d^2) \qquad \text{(II.5)}$$

The counterion entropy is not strong enough to overcome the significant excluded-volume (van der Waals) energy that induces phase separation of the neutral polymer from the solvent. We effectively have a neutral brush, as discussed by Halperin[11] and Zhulina et al.,[12] in these weakly charged regimes. The electrostatic energy acts as a weak perturbation to the brush structure determined principally by excluded-volume effects.

The crossover between the polyelectrolyte and excluded-volume regimes is smooth and continuous below the critical point, the system passing through the Θ regime. However, at higher values of the polyion charge and relatively poorer solvent quality, the line of first-order transitions must be crossed; the collapse transition now occurs abruptly. The discontinuity in the brush thickness at the transition can be estimated by taking the ratio of the scaling results in the polyelectrolyte and excluded-volume regimes.

$$L_p/L_\tau \simeq (\tau d/a)^2 \qquad \text{(II.6)}$$

This is independent of the molecular weight, a feature peculiar to the planar brush, and may easily exceed an order of magnitude.

The polyelectrolyte brush equation of state giving the equilibrium brush thickness L, or equivalently the equilibrium volume fraction ϕ, is found by minimizing the free energy, eq II.2, with respect to L or ϕ. We show the equation of state in Figure 5 for three fixed values of the charge fraction f, taking the excluded-volume parameter τ as the independent variable. The whole range of solvent quality is shown. The lower curve is a subcritical equation of state, $0 < f < f_c$, in which the brush is seen to collapse continuously as the solvent quality is reduced. Note that the brush collapse occurs below the Θ point, where the corresponding neutral brush would have collapsed continuously. The charge serves to renormalize the excluded-volume parameter, reducing the effective Θ point of the

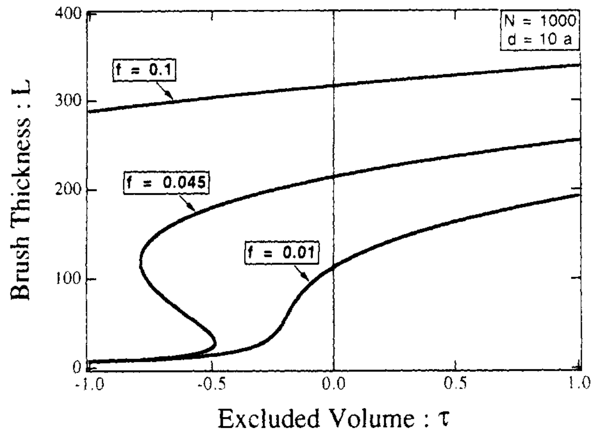

Figure 5. Equations of state for a polyelectrolyte brush. The critical charge fraction is $f_c = 0.02$.

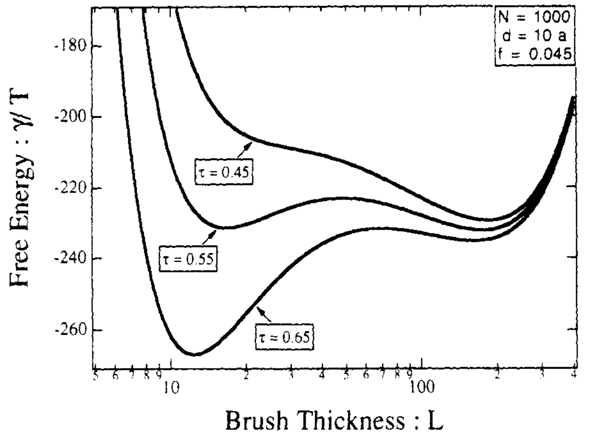

Figure 6. Free energy per chain for a step-function polyelectrolyte brush. The minimum at $L \simeq 200a$ is the electrostatically dominated state. The collapsed minimum develops rapidly as a function of τ, the first-order transition occurring when the two minima have the same free energy.

system. The middle curve is for $f > f_c$ but small enough so as to cross the line of first-order phase transitions. We now have a qualitatively different picture showing a van der Waals like loop in the poor solvent regime, indicative of a mean-field first-order phase transition. The upper curve is for a highly charged polyelectrolyte brush $f \gg f_c$, the equilibrium conformation being nearly independent of solvent quality. Physically, the presence of charge enables the brush to remain in an extended conformation well into the poor solvent regime where the corresponding neutral brush would have already collapsed. In order to induce collapse, the binary attractive interaction must become strong eneough to overwhelm the electrostatic energy and therefore will occur only for very moderately charged brushes as the examples show.

The free energy per chain, eq II.2, is plotted as a function of brush thickness L in Figure 6, for three values of excluded volume τ along the middle equation of state of Figure 5. The minimum at the stretched polyelectrolyte state is the equilibrium state for $\tau < \tau_c$. As we pass through the van der Waals loop, the rapid development of a second minimum at the collapsed state (small L) is seen. The first-order phase transition is the point where the two minima are of equal free energy (middle curve). There is a sizable energy barrier, $\sim 10kT$ per chain, separating the two coexisting states, representing the entropic cost in free energy to reconfigure the polymer system in passing from the solvent-swollen polyelectrolyte state to the solvent-poor collapsed state. Due to this sizable entropy barrier to rearrangements, there should exist nonthermodynamic metastable states in this system. We will comment further on this connection in the Conclusion.

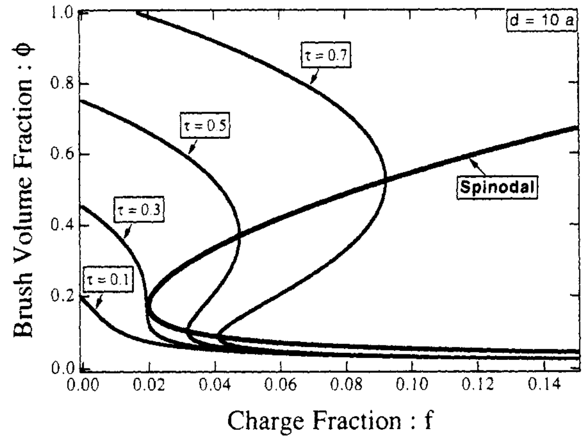

Figure 7. Spinodal curve in the ϕ–f plane (heavy line), along with equations of state for four values of the excluded-volume parameter in the poor solvent regime (thin lines). The critical point is clearly identified.

Finally we show the equation of state, giving the brush volume fraction, for various fixed values of the excluded-volume parameter, both above and below the critical point, taking the charge fraction f as the independent variable, Figure 7. The spinodal, found by setting the second derivative of the free energy equal to zero, is conveniently shown on this plot since its form is independent of the excluded-volume parameter. The upper point on the spinodal is given exactly by $f_s = (3/16)\tau^2$. The first-order phase transition actually occurs at a lower value of f than this, but this value has been consistently used to locate the transition. We remark that Figures 4 and 7 are quite analagous to P–T and P–V diagrams for an ordinary liquid gas coexistence, where f plays the role of a pressure, τ the temperature, and ϕ the volume.

III. Two Opposing Polyelectrolyte Brushes

We now consider the disjoining pressure between two identical opposing Alexander polyelectrolyte brushes with separation $2h$. In the stretched polyelectrolyte regime, for which $f > f_c$ and $\tau^2 < f^*$, the results of Pincus[15] are valid since excluded-volume effects are negligible relative to the electrostatic energy and polymer elasticity. We summarize those results here.

In the limit of very weak or no electrolyte, for which the Debye screening length associated with any added salt is much longer than the brush thickness, $\kappa_s L \ll 1$, the disjoining pressure is exponentially cutoff at distances greater than this screening length κ_s^{-1}, so $\Pi \sim e^{-\kappa_s h}$. Counterion entropy dominates the osmotic pressure for distances greater than the thickness of the polymer layer, $L < h < \kappa_s^{-1}$, so that the disjoining pressure is $\Pi \simeq T/2\pi l h^2$. This is the Gouy–Chapman result for two charged interfaces, due only to the mixing entropy of the counterions. The osmotic pressure of the polyelectrolyte brushes is dominated by the counterions and, hence, so is the disjoining pressure for separations $h < L$, and we find $\Pi \simeq TfN/d^2h$. This is simply the mean counterion density in the compressed layer. Since the osmotic pressure of the counterions in the layer is greater than their associated mixing entropy, the disjoining pressure increases sharply, when the polymer layers come in to contact, over a region of the thickness of the Debye screening length for the highly charged unsalted system $\xi = (4\pi l f c)^{-1/2}$ (see the appendix).

In the excluded-volume-dominated regime, $f < f_c$, and in the collapsed state, $\tau^2 > f^*$, the disjoining pressure is dominated by the excluded-volume terms in the osmotic pressure, $\Pi \simeq T(-(1/2)\tau\phi^2 + (1/3)\phi^3)$, where $\phi = N/d^2h$ is the average monomer density in the compressed layer for $h < L$. The disjoining pressure is again cut off exponentially for $h > L$, with a Debye screening length determined by the counterions $\xi = (4\pi lfc)^{-1/2}$. This is the result found for neutral polymer brushes as discussed in the Introduction, eq I.5, now with the addition of an exponential tail for $h > L$ due to the presence of free counterions.

IV. Cylinders and Spheres

In this section we extend our treatment to the case of polyelectrolyte chains end-grafted to impenetrable cylindrical and spherical surfaces. We are interested in the situation in which the radii of curvature of the surfaces, R_0, is much less than the typical layer height; $R_0 \ll L$. For the alternate case, in which $R_0 \gg L$, the surface layer is locally flat on lengths larger than the brush height and the results of the previous sections for a planar brush apply. The disjoining pressure between two such brushes follows from the Deryaguin approximation.[25]

To calculate the global properties of the brush in these geometries, we follow the approach of Borisov et al.[26] and assume a uniform monomer density in the layer. The grafting density is characterized by the parameter

$$\sigma_\delta = \begin{cases} a^2/\sigma, & \delta = 1 \\ a/h, & \delta = 2 \\ g, & \delta = 3 \end{cases}$$

where σ is the mean surface area per chain on a planar surface ($\delta = 1$); a/h is the number of chains per unit length of the cylinder ($\delta = 2$); and g is the number of chains per sphere ($\delta = 3$). δ denotes the effective dimension of the grafted chains. We take the elastic stretching energy per chain to be that for a uniformly elongated Gaussian polymer. We further assume that the polymer layer remains semidilute so that the chains overlap throughout the entire layer and that the counterions remain localized within the layer. The counterion entropy then still dominates the electrostatic contribution to the total free energy.

We can estimate the validity of this assumption by comparing the effective charge seen on a sphere or cylinder at large distances with the total charge. For the case of a charged sphere, Alexander et al.[27] show that the effective charge is $Z^* \simeq R/l$, up to logarithmic corrections, where R is the radius of the sphere. For the polyelectrolyte sphere considered here, $R = R_0 + L \simeq L$. The total charge on the sphere is just the total polyion charge, $Z = gfN$, so the counterions dominate if $L/l \ll gfN$. In the collapsed state in which we find $L/a \simeq (gN/\tau)^{1/3}$, this condition becomes $f \gg (gN)^{-4/3}\tau^{-2/3}$, which is nearly always satisified. The same calculation for the cylinder yields a similar result.

The free energy per chain thus takes the form

$$\frac{\gamma}{T} \simeq fN \ln\left(\frac{fN\sigma_\delta}{L^\delta}\right) + \left[-\frac{1}{2}\tau\left(\frac{N\sigma_\delta}{L^\delta}\right)^2 + \frac{1}{6}\left(\frac{N\sigma_\delta}{L^\delta}\right)^3\right]\frac{L^\delta}{\sigma_\delta} + \frac{L^2}{2N} \quad \text{(IV.1)}$$

using dimensionless lengths (in units of the monomer size a) and where again δ is the effective dimension of the grafted chains. Minimizing this with respect to L, the layer height, yields a qualitatively similar phase diagram for all three geometries, Figure 4. The critical point is now found at $f_c \simeq N^{-[2(\delta-1)/(\delta+1)]}\sigma_\delta{}^{2/(\delta+1)}$ and $\tau_c \simeq N^{-(\delta-1)/(\delta+1)}\sigma_\delta{}^{1/(\delta+1)}$. In the limit $N \rightarrow \infty$ for the spherical and cylindrical geometries ($\delta = 2$ and 3), the critical point shifts to $f_c = \tau_c = 0$ and the line of first-order phase transitions becomes a line of second-order phase transitions exactly obeying $f^* = (3/16)\tau^2$. The extended electrostatically-dominated regime, for which $L_p \simeq f^{1/2}Na$, lies above the line of phase transitions, $f > f^*$; the collapsed excluded-volume-dominated regime, for which $L_\tau \simeq (N\sigma_\delta/\tau)^{1/\delta}\, a$, lies below. The collapse is much more pronounced in the curved geometries, the collapse ratio scaling as a positive power in N

$$\frac{L_p}{L_\tau} \simeq f^{1/2}\left(\frac{\tau}{\sigma_\delta}\right)^{1/\delta} N^{(\delta-1)/\delta} \quad \text{(IV.2)}$$

Comparison with the results of section II shows that the Θ regime effectively disappears. The phase transition is now very weakly first-order, turning second-order in the infinite N limit. The spinodal of Figure 7 collapses and hence the van der Waals loop in the equation of state disappears along with the entropy barrier in the free energy. The system should no longer give rise to realizable metastable states. The cost in entropy for rearrangement of the layer during the first-order collapse is just made up for in available volume to the chains in the spherical and cylindrical geometries. This additional volume energy does not exist for the planar brush, hence the independence of the critical point on molecular weight and the strong first-order nature of the collapse transition. What appears to happen in the model is that the first-order transition of the charged system coalesces with the coil–globule-like transition of the corresponding neutral system, as described by Borisov et al.,[26] in the limit $N \rightarrow \infty$.

V. Conclusion

In this paper we have investigated the polyelectrolyte brush using an Alexander–de Gennes step-function density profile over the full range of solvent quality. The counterion distribution and electrostatic energy for a planar brush were calculated for a fixed polyion conformation, namely, the step-function profile with a given layer thickness L, using Poisson–Boltzmann theory. The solubility of the polymer backbones was taken into account explicitly by the inclusion of Flory–Huggins mean-field terms in the brush free energy. We find in the poor solvent regime of the corresponding neutral polymer system, for a certain range of grafting densities and polyion charge fraction, a first-order conformational phase transition in which the polyelectrolyte brush collapses discontinuously from an electrostatic and elastically-dominated stretched state to an excluded-volume-dominated collapsed state. In the neighborhood of the phase transition the free energy, Figure 6, displays two minima, one each at the stretched and collapsed states with a sizable energy barrier, $\gg kT$, between them. This barrier indicates the sizable cost in energy to reconfigure the polyelectrolyte brush in the regime where both the stretched and collapsed states are at least metastable.

In a force-balance experiment in which two identical opposing planar polyelectrolyte brushes are compressed together, as discussed in section III, irreversibilities in the disjoining pressure may be expected due to the second minimum in the free energy at the collapsed state. Starting with both brushes in the stretched state, the force-balance apparatus would provide the needed energy to get the brushes over the thermal barrier into the collapsed minimum. The measured disjoining pressure will then be seen to vanish at a much smaller separation. All subsequent compressions of the brushes will show a disjoining pressure curve characteristic of a collapsed Halperin brush.

If the stretched minimum is the global minimum of the free energy, the collapsed minimum being only metastable, the brush may return to the stretched state via thermal fluctuations over the compact layer. The disjoining pressure curve for the next compression will then be that for a stretched, electrostically-dominated brush once again. The relaxation time associated with this behavior is expected to be fairly sensitive to solvent quality (temperature) and charge fraction (pH) as the barrier height and relative depth of the two energy minima vary over a relatively small range of these parameters. This type of behavior has indeed been observed by Klein and Luckham[28-30] and Argillier and Tirrell.[31] Whether or not these observations are related to the competition between counterion swelling and poor solvent collapse requires further study.

The extension of this model to the case of end-grafted polyelectrolytes on spherical and cylindrical surfaces shows that the planar brush is unique in that the molecular weight plays no role in determining the phase behavior besides setting the lower limit on the grafting density in the brush regime. For these curved geometries, we still find a first-order collapse transition from the electrostatic and elastically-dominated stretched state to the excluded-volume-dominated "globule" state. The phase transition is now only weakly first-order. The existence of metastable states is unlikely, and in the limit $N \rightarrow \infty$ the phase transition becomes second-order. The collapse ratio is also much larger, scaling with molecular weight $L_p/L_r \sim N^{(\delta-1)/\delta}$, where δ is the effective dimension of the grafted chains.

A few questions remain about the simple treatment used for these curved geometries. For very long grafted polyelectrolytes there should certainly be a corona of nonoverlapping rodlike polyelectrolytes. How thick this corona is and how it collapses in poor solvent is not clear. It may, for instance, undergo a Khokhlov like collapse, possibly involving an avalanche counterion condensation.[32] This type of collapse is continuous, occurring as a coil–globule transition with a relatively short correlation length, i.e., on the scale of individual electrostatic blobs. How this effects the collapse of the underlying semidilute layer requires further study.

In a previous paper,[15] Pincus remarked on the effects of added electrolyte on the polyelectrolyte brush. That treatment was based on the assumption that the swelling pressure in the layer was simply the osmotic pressure of a semidilute polyelectrolyte solution in the presence of added electrolyte as derived by Witten and Pincus.[33] It is not clear, however, that this simple approach is correct since the electrostatic interaction in the strongly charged polyelectrolyte brush is already highly screened even in the absence of salt for $\xi \ll L$. There should certainly be a crossover to a regime at high salt concentration in which the chains behave like grafted wormlike polymers displaying electrostatic excluded-volume effects.[34]

To find the conformation of the planar brush in this extreme case, we balance the osmotic pressure of Odijk chains against the Gaussian elasticity of a persistent chain. The persistence length is taken to be the Odijk length $L_e = l/4(a/f)^2\kappa^2$ (the chain is assumed Gaussian in the absence of electrostatic interactions) and the electrostatic excluded-volume parameter is $\upsilon_{el} \simeq L_e^2/\kappa$. The osmotic pressure supporting the brush is therefore $\Pi/T \simeq (1/2)\upsilon_{el}c_r^2$, where $c_r = ca/L_e$ is the concentration of rodlike segments in the layer. The elastic energy of the persistent chain is $L^2/2NaL_e$. Static equilibrium is governed by

$$\Pi/T = \frac{L^2}{2NaL_e}\frac{1}{Ld^2} \qquad (V.1)$$

which yields for the layer thickness

$$L \simeq \frac{N}{2\kappa}\left(\frac{f^2la}{d^2}\right)^{1/3} \qquad (V.2)$$

This description is valid so long as the monomer concentration is less than the cube of the inverse Debye length $c \ll \kappa^3 \simeq (8\pi lc_s)^{3/2}$. Using L calculated above and $c = N/d^2L$, we find the lower limit on this high salt regime

$$c_s > (4\pi f^{2/3}(lda)^{1/3}ld)^{-1} \qquad (V.3)$$

Although the very low and very high salt limits are obtainable, the correct approach for treating added electrolyte in dense polyelectrolyte systems with restricted geometries, such as that discussed in this paper, eludes us at present. One thing does seem clear however; due to the additional screening of the bare electrostatic interaction, which can be thought of as a reduction of the effective charge fraction, a polyelectrolyte brush near (and above) the phase transition should undergo a discontinuous electrolyte-induced collapse. The scenario for a highly charged polyelectrolyte brush far from the phase transition, in the presence of added electrolyte, may be quite different. Work in this area will be presented in a future paper.

We finally remark on the applicability of the step-function ansatz. In this paper we focused on the global properties of the system. In particular, we simply analyzed the competition between electrostatic energy, tending to swell the brush, and excluded-volume (van der Waals) energy, tending to collapse the brush in the poor solvent regime for the neutral polymer backbones. The deviation of the polymer density profile from the assumed step-function form should not effect our results in any significant way. Even with a self-consistent density profile[13,14] the brush is highly solvent swollen and we expect the counterions to be confined to the layer, their localization entropy still dominating the swelling osmotic pressure. For moderately charged polyelectrolytes, the insolvency effects of poor solvent remain due to exposed neutral polymer segments, and a collapse transition should indeed occur. Since the brush is relatively dense and presumably highly entangled, the entropic cost of rearrangement of the layer in order to collapse is still sizable and the transition is expected to remain strongly first-order. For the cylindrical and spherical geometries, the step-function ansatz is perhaps more believable. In any case, the competition between forces of opposite sign remains and a phase transition is still expected. In these cases it is more likely second-order due to the additional volume per chain, essentially eliminating the entropic barrier to rearrangements.

We have demonstrated then that, within the mean-field approximation for the electrostatic and excluded-volume interactions, the Alexander profile polyelectrolyte brush exhibits a first-order conformational phase transition in the poor solvent regime of the corresponding neutral polymer system. The existence of metastable states associated with this phase transition for the planar brush is predicted to be demonstrable through irreversibilities in the disjoining pressure measured in force-balance experiments in which two identical polyelectrolyte brushes are compressed together.

Acknowledgment. We express our sincere thanks to E. B. Zhulina, J.-F. Argillier, M. Tirrell, J. Klein, and J.

Israelachvili for many helpful discussions. This work was supported in part by SURS Grant No. 0357(800612) from IBM and the U.S. DOE Grant No. DE-FG03-87ER45288.

Appendix

This appendix provides the details of the calculation of the electrostatic energy of an Alexander–de Gennes profile polyelectrolyte brush. This is a review of results already presented,[15] including the details relevant to this work.

Consider polyelectrolyte chains having degree of polymerization N and charging fraction f end-grafted to a flat surface with mean spacing d. Assuming translational invariance on the grafting surface, i.e., no lateral polymer or charge density fluctuations, reduces this to an effective one-dimensional problem. For charging fractions small enough so as not to induce Manning condensation[35] (not a strong restriction), the counterions form a surface layer with charge density found by solving the Poisson–Boltzmann equation for the electrostatic potential $\Phi(x)$

$$\frac{\mathrm{d}^2\phi}{\mathrm{d}x^2} = 4\pi l[fc(x) - \rho_+ e^{-\phi(x)}] \tag{A.1}$$

where the dimensionless potential $\phi = e\Phi/kT$ is employed, $\rho_+ e^{-\phi(x)}$ is the local counterion distribution, $fc(x)$ is the local charged monomer density, and $l = e^2/\epsilon kT$ is the Bjerrum length. Using a step-function profile $c(x) = (N/Ld^2)\Theta(L - x)$, the solution in the outer region $x > L$ is simply the Gouy–Chapman solution for a charged interface at L with surface potential $\phi_L = \phi(L)$

$$\phi(x) = 2 \log \left[e^{\phi_L/2} + \frac{x - L}{\xi}\right] \tag{A.2}$$

where $\xi = (4\pi l\rho_+)^{-1/2}$. In the brush region, $x < L$, the potential is found implicitly as the solution of the integral equation

$$\frac{2x}{\xi} = \int_0^{\phi} \frac{\mathrm{d}\phi}{\left(e^{-\phi} - 1 + \dfrac{\phi}{\phi_L}\right)^{1/2}} \tag{A.3}$$

Continuity of the electric field at L gives $\phi_L = \rho_+/c$. It is interesting to note that analyticity of eq A.3 for small values of the potential requires $\phi_L \leq 1$. This means that the electrostatic energy per charged monomer can never exceed kT, for otherwise the system will self-adjust by stretching until this condition is met.

In the limit of weak charging $\phi_L \ll 1$, eq A.3 gives the result $\phi_L \simeq L/\xi$, where the counterion screening length $\xi = d^2/2\pi lfN$ is simply the Gouy–Chapman length for a charged interface. Hence, $L < \xi$ and we do not expect electrostatics to play a large role in determining the brush conformation. For strong charging in which $\phi_L \simeq 1$, we obtain the self-consistent solution $\phi_L \simeq 1 - e^{-2^{1/2}L/\xi}$. Thus, $L \gg \xi$ and electrostatics are expected to play a significant role. The counterions localize to within a distance ξ of the charged monomers on average, effectively pinning them to the polymer component of the brush. The screening length can then be found by appealing to local charge neutrality with the result $\xi = (4\pi lfc)^{-1/2}$.

Using these results, we can now find the electrostatic free energy by formally integrating the free energy density, which consists of the electrostatic energy of the charged chains and counterions in the potential $\phi(x)$, and the counterion entropy

$$\frac{F_{\text{es}}}{T} = \frac{1}{2}(\rho_+ e^{-\phi} - c)\phi + \rho_+ e^{-\phi} \log (\rho_+ e^{-\phi}) \tag{A.4}$$

We do not need to know $\phi(x)$ explicitly to find the integrated free energy per unit area on the grafting surface in the two charging limits, and we obtain

$$\frac{\gamma_{\text{es}}}{T} \simeq \begin{cases} fcL \log (fc), & \text{strong charging} \\ -\frac{1}{6}fcL^2/\xi, & \text{weak charging} \end{cases}$$

In the absence of excluded-volume effects, the balance of γ_{es} and chain elasticity, which we take to be that for stretched Gaussian chains $L^2/2Na^2d^2$, gives the equilibrium brush heights $L = f^{1/2}Na$ and $L = (\pi/3)f^2N^3l(a/d)^2$, respectively, and the value of f where the crossover from weak to strong charging occurs is $f \simeq (d^2/N^2la)^{2/3}$. The electrostatic screening length in the strong charging limit becomes $\xi = d(a/4\pi lf^{1/2})^{1/2}$, using the explicit form for L.

References and Notes

(1) Alexander, S. *J. Phys. (Paris)* **1977**, *38*, 983.
(2) de Gennes, P.-G. *Macromolecules* **1980**, *13*, 1069.
(3) Milner, S. T.; Witten, T. A.; Cates, M. E. *Europhys. Lett.* **1989**, *5*, 413.
(4) Milner, S. T.; Witten, T. A.; Cates, M. E. *Macromolecules* **1988**, *21*, 2610.
(5) Milner, S. T. *Europhys. Lett.* **1988**, *7*, 695.
(6) Birshtein, T. M.; Zhulina, E. B. *Polym. Sci. USSR* **1983**, *25*, 2165.
(7) Birshtein, T. M.; Zhulina, E. B. *Polymer* **1984**, *25*, 1453.
(8) Zhulina, E. B. *Polym. Sci. USSR* **1984**, *26*, 885.
(9) Borisov, O. B.; Zhulina, E. B.; Birshtein, T. M. *Vysokomol. Soedin.* **1988**, *A30*, 767.
(10) Skovortsov, A. M.; Pavlushkov, I. V.; Gortimov, A. A.; Zhulina, E. B.; Borisov, O. V.; Pryamitsyn, V. A. *Vysokomol. Soedin.* **1988**, *A30*, 1615.
(11) Halperin, A. *J. Phys. (Paris)* **1988**, *49*, 547.
(12) Zhulina, E. B.; Borisov, O. B.; Pryamitsyn, V. A.; Birshtein, T. M. *Macromolecules* **1991**, *24*, 140.
(13) Miklavic, S. J.; Marčelja, S. *J. Phys. Chem.* **1988**, *92*, 6718.
(14) Misra, S.; Varanasi, S.; Varanasi, P. P. *Macromolecules* **1989**, *22*, 4173.
(15) Pincus, P. *Macromolecules* **1991**, *24*, 2912.
(16) Davis, R. M.; Russel, W. B. *J. Polym. Sci.* **1986**, *B24*, 511.
(17) Joanny, J. F.; Leibler, L. *J. Phys. (Paris)* **1990**, *151*, 545.
(18) Borisov, O. V.; Birshtein, T. M.; Zhulina, E. B. *J. Phys. II* **1991**, *1*, 521.
(19) Tanaka, T.; Fillmore, D.; Sun, S.; Nishio, I.; Swislow, G.; Shah, A. *Phys. Rev. Lett.* **1980**, *45*, 1636.
(20) Ohmine, I.; Tanaka, T. *J. Chem. Phys.* **1982**, *77*, 5725.
(21) Throughout this paper we assume that the grafting density is sufficiently high that the mean spacing, d, is smaller than the characteristic polymer dimension. This implies that the local polymer concentration is in the semidilute (or denser) range.
(22) de Gennes, P.-G. *Scaling Concepts in Polymer Physics*; Cornell University Press: Ithaca, NY, 1979.
(23) Throughout this paper we assume that the magnitude of the two-body interaction, τ, is sufficiently small that the polymer concentrations are still in the dilute range, $\phi \ll 1$, so that the virial expansion of eq I.1 is meaningful.
(24) The monomer concentration for neutral polymers in good solvents is known to be distributed parabolically.[3,4,10,36] However, the Alexander approximation of assuming that the ends all lie at the extent of the brush yields the correct scaling behavior which is of interest here.
(25) Israelachvili, J. N. *Intermolecular and Surface Forces*; Academic Press: London, 1985.
(26) Borisov, O. V.; Zhulina, Ye. B.; Birshtein, T. M. *Polym. Sci. USSR* **1988**, *30*, 772.
(27) Alexander, A.; Chaikin, P. M.; Grant, P.; Morales, G. J.; Pincus, P.; Hone, D. *J. Chem. Phys.* **1984**, *80*, 5776.
(28) Klein, J.; Luckham, P. F. *Macromolecules* **1984**, *17*, 1041.
(29) Luckham, P. F.; Klein, J. *J. Chem. Soc.; Faraday Trans. 1* **1984**, *80*, 865.
(30) Klein, J.; Luckham, P. F. *Colloids Surf.* **1984**, *10*, 65.
(31) Argillier, J.-F.; Tirrell, M., private communication.
(32) Khokhlov, A. R. *J. Phys. A* **1980**, *13*, 979.
(33) Witten, T. A.; Pincus, P. *Europhys. Lett.* **1987**, *3*, 315.
(34) Odijk, T.; Houwaart, A. C. *J. Polym. Sci., Polym. Phys. Ed.* **1978**, *16*, 627.
(35) Manning, G. *J. Chem. Phys.* **1969**, *51*, 924.
(36) Hirz, S. J. Modeling of Interactions Between Adsorbed Block Copolymers. M.s. Thesis, University of Minnesota, Minneapolis, MN, 1988.